

See discussions, stats, and author profiles for this publication at: <https://www.researchgate.net/publication/230833497>

Discovery of Small-Molecule Inhibitors of the TLR1/TLR2 Complex

ARTICLE *in* ANGEWANDTE CHEMIE INTERNATIONAL EDITION · DECEMBER 2012

Impact Factor: 11.26 · DOI: 10.1002/anie.201204910 · Source: PubMed

CITATIONS

18

READS

55

4 AUTHORS, INCLUDING:



Xiaohui Wang

Chinese Academy of Sciences

40 PUBLICATIONS 1,060 CITATIONS

SEE PROFILE



Hang Yin

University of Colorado Boulder

113 PUBLICATIONS 2,808 CITATIONS

SEE PROFILE



Discovery of Small-Molecule Inhibitors of the TLR1/TLR2 Complex**

Kui Cheng, Xiaohui Wang, Shuting Zhang, and Hang Yin*

Toll-like receptors (TLRs) are type I transmembrane proteins that recognize pathogen-derived macromolecules and play a key role in the innate immune system.^[1–3] The pathogen-derived macromolecules, which are broadly shared by pathogens but distinguishable from host molecules, are collectively referred to as pathogen-associated molecular patterns (PAMPs).^[1,4] In humans, 10 TLRs respond to a variety of PAMPs, including a lipopolysaccharide (TLR4), lipopeptides (TLR2 associated with TLR1 or TLR6), bacterial flagellin (TLR5), viral double-stranded (ds)RNA (TLR3), viral or bacterial single-stranded (ss)RNA (TLRs 7 and 8), and cytidine-phosphateguanosine (CpG)-rich unmethylated DNA (TLR9), among others.^[5–7]

TLR dimerization leads to the activation of nuclear factor- κ B (NF- κ B) and interferon-regulatory factors (IRFs), and these transcription factors in turn induce the production of pro-inflammatory cytokines and type I interferons (IFNs), respectively.^[1,8] Finally, the key outputs from TLR activation are inflammatory cytokines such as tumor necrosis factor (TNF) and interleukin 1 β (IL-1 β), which have proven to be directly relevant to inflammatory diseases.^[9] TLR2, signaling as a heterodimer with either TLR1 or TLR6, recognizes a wide range of ligands, many of which are from Gram-positive bacteria.^[10] The molecular recognition by TLR2 was largely explained when the crystal structure of the TLR1/TLR2 heterodimer in complex with its specific lipoprotein ligand, Pam₃CSK₄, was solved.^[11] In this structure (Figure S1a in the Supporting Information), the extracellular domains of TLR1 and TLR2 form an M-shaped heterodimer, with the two N termini extending outward in opposite directions. The lipid chains of Pam₃CSK₄ bridge the two TLRs, contributing to the formation of the heterodimer. Two of the three lipid chains of Pam₃CSK₄ interact with a hydrophobic pocket in TLR2, and the amide-bound lipid chain lies in a hydrophobic channel within TLR1. The ligand-bound complex of TLR1 and TLR2 is stabilized by protein–protein contacts near the ligand-binding pocket.^[9,11]

Previous reports have demonstrated that the cytokine response to human cytomegalovirus (CMV), lymphocytic choriomeningitis virus (LCMV), and herpes simplex virus 1

(HSV-1) is regulated by TLR1/TLR2.^[12,13] TLR1/TLR2 antagonists have been suggested to have beneficial effects in both chronic and acute inflammatory diseases ranging from acne^[12] to sepsis,^[13] and can also attenuate pulmonary metastases of tumors.^[14] However, a significant bottleneck in the field can be attributed to the lack of efficient and specific probes for the TLR1/TLR2 signaling pathway. Even though the limited success of TLR2 regulators has been reported in literature,^[15] low-molecular-weight inhibitors with high potency and specificity against TLR1/TLR2 have not been reported to our knowledge.

Novel inhibitors of TLR1/TLR2 were obtained by cell-based screening of the small-molecule library *NCI-2 Diversity* consisting of 1363 compounds. Screening was performed in a 96 well plates format using our previously established high-throughput nitric oxide (NO) assay in RAW264.7 macrophage cells (details on the screening method are given in Figure S2 in the Supporting Information).^[16,17] Synthetic triacylated lipoprotein Pam₃CSK₄ was employed to selectively activate TLR1/TLR2 signaling, resulting in the expression of inducible nitric oxide synthase (iNOS) and the production of NO in RAW264.7 macrophage cells.^[16] We monitored the NO level as an indicator of Pam₃CSK₄-induced TLR1/TLR2 activation to determine the potency of the inhibitors.

We identified nine initial hits (Scheme S1 in the Supporting Information) that inhibited TLR1/TLR2 activation by at least 70 % at 3.0 μ M with no significant cytotoxicity (Figure S3 in the Supporting Information). The most potent compound was NCI35676 (Table 1, a natural product named purpurogallin obtained from nutgalls and oak bark) with an IC₅₀ of (2.45 \pm 0.25) μ M (Figure S4 in the Supporting Information). NCI35676 has been reported to display antioxidant^[18] and anticancer^[19,20] properties, and it also modulates inflammatory response activity.^[21] Nonetheless, work on the molecular target of purpurogallin and its derivatives has not yet been reported. Further, when we evaluated TLR specificity we found that of the nine initial hits, only NCI35676 specifically inhibited TLR1/TLR2 signaling but not that of other homologous TLRs (Figure S5 in the Supporting Information).

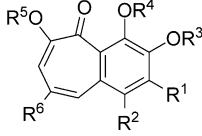
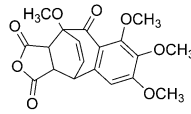
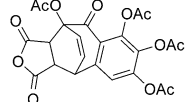
Based on the promising preliminary results, we attempted to optimize the structure of NCI35676 to improve its inhibitory potency and selectivity. We designed a series of NCI35676 analogues to explore the structure–activity relationship (SAR) around the benzotropolone core scaffold. A one-pot synthesis with sequential additions of a) phosphate-citrate buffer (pH 5), b) horseradish peroxidase enzyme, c) 3 % H₂O₂ produced the bicyclic scaffold (Scheme 1 and Scheme S2 in the Supporting Information).^[22] This method provides a concise, general synthetic route that can afford the benzotropolone derivatives with an overall yield of 15–60 %. Compound **2** was selected as a representative for further

[*] Dr. K. Cheng, Dr. X. H. Wang, S. T. Zhang, Prof. Dr. H. Yin
Department of Chemistry and Biochemistry
and the BioFrontiers Institute
University of Colorado at Boulder, Boulder, CO 80309 (USA)
E-mail: hubert.yin@colorado.edu

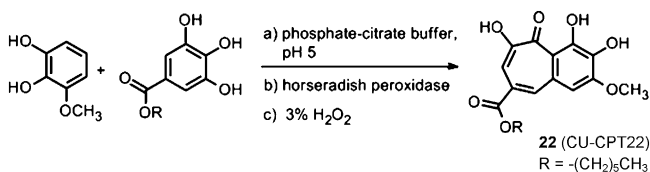
[**] We thank the U.S. National Institutes of Health (DA026950, DA025740s and NS067425) for financial support of this work. The sTLR2 DNA plasmid was kindly provided by Dr. Chiaki Nishitani and Dr. Yoshio Kuroki.

Supporting information for this article is available on the WWW under <http://dx.doi.org/10.1002/anie.201204910>.

Table 1: Analysis of the structure–activity relationship of the benzotropolone analogues for the inhibition of NO production in RAW 264.7 cells.

					
	1: $R^2 = \text{CH}_3, R^6 = \text{H}$ 2–9, NCI35676: $R^2 = R^6 = \text{H}$ 10–24: $R^2 = R^3 = R^4 = R^5 = \text{H}$				
Compound	R ¹	R ³	R ⁴	R ⁵	IC ₅₀ [μM] ^[a]
NCI35676	OH	H	H	H	2.45 ± 0.25
1	H	H	H	H	3.13 ± 0.11
2	H	H	H	H	2.25 ± 0.31
3	F	H	H	H	22.7 ± 1.4
4	OCH ₃	H	H	H	4.83 ± 0.25
5	OCH ₃	CH ₃	H	CH ₃	11.7 ± 1.1
6	OCH ₃	CH ₃	CH ₃	CH ₃	39.9 ± 0.9
7	OCOCH ₃	H	H	H	4.83 ± 0.25
8	OCOCH ₃	COCH ₃	H	COCH ₃	1.42 ± 0.21
9	OCOCH ₃	COCH ₃	COCH ₃	COCH ₃	2.35 ± 0.41
	R ¹	R ⁶			
10	OCH ₃	COOH			21.5 ± 0.4
11	OCH ₃	COOCH ₃			3.11 ± 0.75
12	H	COOH			16.5 ± 0.8
13	H	COOCH ₃			9.01 ± 0.50
14	OCH ₃	COOCH ₂ CH ₃			2.83 ± 0.44
15	OCH ₃	COOCH(CH ₃) ₂			2.47 ± 0.71
16	OCH ₃	COO(CH ₂) ₃ CH ₃			2.83 ± 0.44
17	OCH ₃	COO(CH ₂) ₇ CH ₃			0.72 ± 0.14
18	OCH ₃	COO(CH ₂) ₉ CH ₃			1.01 ± 0.10
19	OCH ₃	COO(CH ₂) ₁₃ CH ₃			3.24 ± 0.13
20	OCH ₃	CONH(CH ₂) ₃ CH ₃			1.26 ± 0.31
21	OCH ₃	CONH(CH ₂) ₅ CH ₃			1.36 ± 0.21
CU-CPT22	OCH ₃	COO(CH ₂) ₅ CH ₃			0.58 ± 0.09
23	OCH ₃	CH ₂ OH			4.11 ± 0.74
24	OCH ₃	CONH(<i>o</i> -tolyl)			1.36 ± 0.21
25					74.6 ± 2.9
26					14.8 ± 0.5

[a] IC₅₀ values and corresponding standard deviations were determined from at least three independent repeats.



Scheme 1. One-pot synthesis of CU-CPT22: a) phosphate–citrate buffer (pH 5), 0.2 M Na₂HPO₄/0.1 M citrate (1:1); b) horseradish peroxidase; c) four aliquots of 3 % H₂O₂, 42 % overall yield.

NMR characterizations (¹H/¹³C, HSQC, HMBC, and COSY included in Figure S6 in the Supporting Information).

Further screening of 26 structural analogues yielded additional hits, the most potent being CU-CPT22, which showed an IC₅₀ of (0.58 ± 0.09) μM (Figure 1 a). The improved IC₅₀ of CU-CPT22 appears to be due to the addition of a six-

carbon aliphatic chain at the R⁶ position, which likely allows for hydrophobic contacts to the surface residues of the TLR1/TLR2 complex (Figure 1 b).

The SAR for this series indicated that the total number of hydroxy groups was critical. Methylation of one hydroxy group at the R¹ position (**4**) had a modest effect on its activity, while methylation of all four hydroxy groups (**6**) resulted in significant decrease of inhibition (Table 1). Introduction of a fluorine substituent at the R¹ position (**3**) decreased the activity about 20-fold, suggesting that an electron-withdrawing group is not favorable here. We also found that the seven-membered-ring configuration in the benzotropolone scaffold plays an important role for inhibitory activity as determined by the Diels–Alder [4+2]-cycloaddition products (**6** versus **25**, **9** versus **26**).

We found that conversion of the hydroxy group at R¹ to a methoxy group eliminated the formation of by-products, but still retained the activity of NCI35676 (Scheme S2 in the Supporting Information). Therefore, in the following SAR studies, the methoxy group was fixed at the R¹ position. Meanwhile, the seven-membered ring in the benzotropolone scaffold was kept and substituent groups were introduced at the R⁶ position. The addition of a carboxyl group at the R⁶ position decreased the activity by approximately fivefold (**4** versus **10**), while esterification of this carboxyl group (**11**) returned the activity to the NCI35676 level, indicating that R⁶ may be critical for the inhibitory activity.

By introducing various aliphatic chains at the R⁶ position, we found that CU-CPT22 with a six-carbon chain displayed the highest inhibitory activity for TLR1/TLR2 (Table 1). This increased potency was likely caused by a good fit of the six-carbon chain into the substrate tunnel of the TLR1 hydrophobic region (Figure 1 b). When we replaced the ester with the amide group at the R⁶ position in CU-CPT22, the activity slightly decreased (**21**). Reducing the carboxyl group to a -CH₂OH group (**23**) or introducing a large substitute at the R⁶ position (**24**) led to no significant change in activity. In summary, we identified compound CU-CPT22 as the lead structure, which shows dose-dependent inhibitory effects in blocking Pam₃CSK₄-induced TLR1/TLR2 activation with an IC₅₀ of (0.58 ± 0.09) μM (Figure 1 a).

Biophysical tests were carried out for CU-CPT22, along with the negative control compound **6**, to demonstrate that CU-CPT22 directly binds to TLR1/TLR2. The TLR2 protein was expressed in the baculovirus insect cell expression system using the methods described by Kuroki and co-workers.^[24] The activities of the TLR2 and TLR1 protein were validated by the fluorescence anisotropy assay with the rhodamine-labeled, synthetic triacylated lipoprotein Pam₃CSK₄ as the probe (Figure 2 a). It was demonstrated that CU-CPT22 was able to compete with Pam₃CSK₄ for binding to TLR1/TLR2 with an inhibition constant (K_i) of (0.41 ± 0.07) μM, which is consistent with its potency observed in the whole-cell assay. The anisotropy of rhodamine-labeled Pam₃CSK₄ showed a robust increase from 0.168 to 0.275 (Figure 2 a) upon addition of TLR1/TLR2 (excitation = 549 nm; emission = 566 nm). This increase is consistent with the anisotropy changes seen with ligand–receptor pairs of comparable sizes.^[25] Increasing the concentration of CU-CPT22 to 6 μM

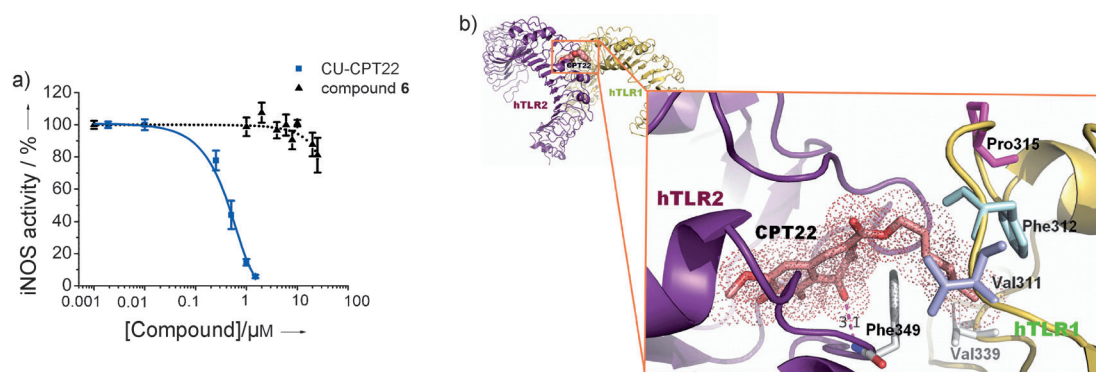


Figure 1. a) Dose-dependent inhibition of NO production in RAW264.7 macrophage cells by CU-CPT22 and the negative control compound **6**. b) Binding site of CU-CPT22 (shown in the stick representation) in TLR1/TLR2 predicted by the program Glide 5.6.^[23] The six-carbon chain fits well into the hydrophobic channel of hTLR1 and has key hydrophobic interactions with Val311, Phe312, Pro315, and Val339.

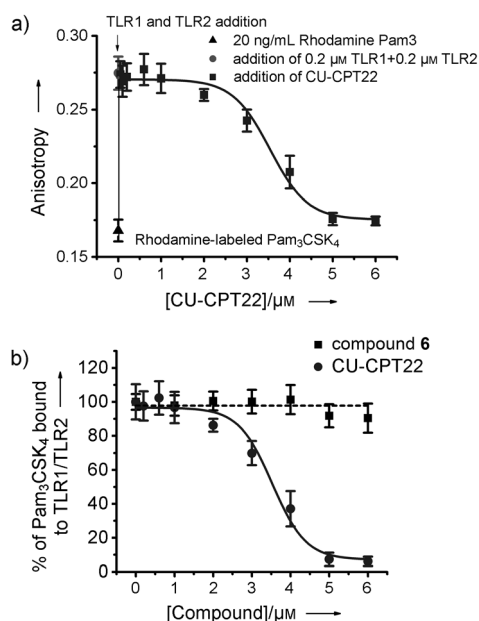


Figure 2. Fluorescence anisotropy titration: a) titration of the TLR1/TLR2 protein into the rhodamine-labeled Pam₃CSK₄ results in a significant increase of fluorescence anisotropy. Added CU-CPT22 competes with Pam₃CSK₄ and results in lower fluorescence anisotropy; this demonstrates competitive binding between CU-CPT22 and Pam₃CSK₄ for TLR1/TLR2. Data were fitted using a one-site competition model ($R^2 > 0.98$). b) Normalized binding of CU-CPT22 compared with the negative control, compound **6**.

decreased the anisotropy to background levels, presumably because of the release of the fluorescently labeled Pam₃CSK₄ probe. This data was then fit to a one-site competition model. From the good fit ($R^2 > 0.98$) we infer that CU-CPT22 and Pam₃CSK₄ compete for the same binding site on the surface of the TLR1/TLR2 heterodimer. By contrast, compound **6**, which was used as a negative control in the anisotropy assay, demonstrated negligible binding up to 6 μM (Figure 2b). These results further support the premise that CU-CPT22 can compete with Pam₃CSK₄ binding to TLR1/TLR2.

One challenge in developing inhibitors to target TLRs is to engineer specificity and potency. There are at least 13 homologous TLRs present in murine macrophages, all shar-

ing a ligand-binding domain with a double-horseshoe shape.^[7] We therefore tested CU-CPT22 against a panel of homologous TLRs, including TLR1/TLR2, TLR2/TLR6, TLR3, TLR4, and TLR7 using TLR-specific ligands to selectively activate a particular TLR-mediated NO production. We found that CU-CPT22 inhibits TLR1/TLR2 signaling without affecting other TLRs, showing that it is highly selective in intact cells (Figure 3).

Importantly, CU-CPT22 was found to have no significant cytotoxicity at various concentrations up to 100 μM in RAW264.7 cells using the established MTT methodology (Figure S7 in the Supporting Information). Furthermore, kinase profiling showed that compound CU-CPT22 demonstrated minimal nonspecific inhibition against a panel of 10 representative kinases (PDGFRB, MET, DDR2, SRC, MAPK1, PAK1, AKT1, PKC- γ , CAMK1, and PLK4) (Figure S8 in the Supporting Information). Lastly, we used a secondary cellular assay to confirm that CU-CPT22 also inhibits the downstream signaling transduction. In addition to the suppression of NO production, we also investigated the release of the proinflammatory cytokines TNF- α and IL-1 β , which are also regulated by the TLR1/TLR2 signaling

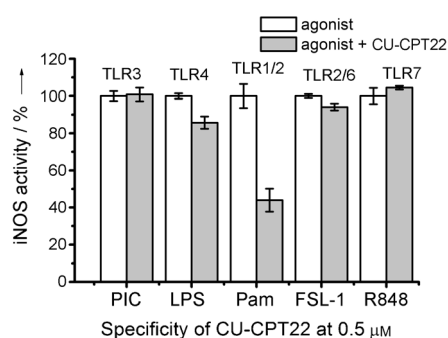


Figure 3. Specificity test for CU-CPT22 (0.5 μM) with TLR-specific agonists used to selectively activate the respective TLRs: 1. TLR3: 15 $\mu\text{g mL}^{-1}$ polyinosinic-polycytidylic acid (PIC), 2. TLR4: 10 ng mL^{-1} lipopolysaccharide (LPS), 3. TLR1/TLR2: 200 ng mL^{-1} Pam₃CSK₄, 4. TLR2/TLR6: 10 ng mL^{-1} (S,R)-(2,3-bisphosphatidyl)-Cys-Gly-Asp-Pro-Lys-His-Pro-Lys-Ser-Phe (FSL-1), and 5. TLR7: 100 nm 4-amino-2-(ethoxymethyl)- α (R848) were used to selectively activate respective TLRs.

